

## Magnetic Circular Dichroism in Resonant Raman Scattering in the Perpendicular Geometry at the $L$ edge of $3d$ Transition Metal Systems

L. Braicovich,<sup>1,2</sup> G. van der Laan,<sup>3</sup> G. Ghiringhelli,<sup>4</sup> A. Tagliaferri,<sup>1,2</sup> M. A. van Veenendaal,<sup>5</sup> N. B. Brookes,<sup>4</sup>  
M. M. Chervinskii,<sup>6</sup> C. Dallera,<sup>1</sup> B. De Michelis,<sup>1,2</sup> and H. A. Dürr<sup>3</sup>

<sup>1</sup>*INFM, Istituto Nazionale di Fisica della Materia, Italy*

<sup>2</sup>*Dipartimento di Fisica del Politecnico, P.L. da Vinci 32, 20133 Milano, Italy*

<sup>3</sup>*Daresbury Laboratory, Warrington WA4 4AD, United Kingdom*

<sup>4</sup>*European Synchrotron Radiation Facility, BP 220, 38043 Grenoble, France*

<sup>5</sup>*Materials Science Division, Argonne National Laboratory, 9700 South Cass Avenue, Argonne, Illinois 60439*

<sup>6</sup>*D. I. Mendeleev Institute for Metrology, 19 Moskovsky Prospekt, 198005 Skt. Petersburg, Russia*

(Received 22 April 1998)

We measured circular dichroism in resonant x-ray scattering  $3d^n \rightarrow 2p^5 3d^{n+1} \rightarrow 3s^1 3d^{n+1}$  with incidence perpendicular to the magnetization where the absorption dichroism vanishes. The advantages of photon scattering over other techniques make it possible to study a wide range of materials. The Ni  $L_3$  dichroism in  $\text{NiFe}_2\text{O}_4$  is  $(28 \pm 5)\%$  in agreement with a localized model. In the metal Co the dichroism is reduced to  $(10.4 \pm 1)\%$  ( $L_3$ ) and  $(6.8 \pm 1.5)\%$  (7.5 eV above  $L_3$ ), indicating a large sensitivity to the nature of the valence states despite the fact that this spectroscopy is based on inner shell transitions. [S0031-9007(99)08431-8]

PACS numbers: 78.70.En, 78.70.Ck, 78.70.Dm

In recent years there has been a considerable effort in circular x-ray dichroism on magnetic materials [1], which provides important, and in many aspects unique, information especially by the use of the sum rules [2]. Much of this effort has been devoted to dichroism in x-ray absorption exploiting the difference in the number of the created core holes for parallel and antiparallel alignment of the magnetization and helicity vector of the incident light. The charge distribution of the excited core hole is not only characterized by its integral which is proportional to the absorption but also by its spatial distribution which is in general not spherical. Information on the deviation from the spherical symmetry, i.e., on the core hole polarization can be obtained from the angular dependence of the particles emitted by the decay of the core hole [3,4]. Since this deviation is directly connected to the ground state properties by the optical transition matrix elements of the absorption process, important information about the material properties is laying dormant in the angular emission when only absorption is measured. The dichroism in absorption vanishes when the incident light is perpendicular to the magnetization, i.e., in the so-called “forbidden” geometry. Let us consider the plane defined by the incident beam and by the emitted products detected in the experiment, with the magnetization in this plane (coplanar perpendicular geometry hereafter referred to as “perpendicular”). The detection breaks the mirror symmetry of the system, and one obtains information on the nonspherical part of the core hole distribution. So far this approach has been used only in experiments based on electron emission [3,5]. The possibility of detecting emitted photons has never been explored. The aim of the present Letter is not only to show that this is feasible but to present original results in this field. We concentrate on

$3d$  TM systems, and we use the inner shell excitation of the type  $3d^n \rightarrow 2p^5 3d^{n+1} \rightarrow 3s^1 3d^{n+1}$  (i.e., final state with a  $3s$  hole due to the filling of the intermediate  $2p$  core hole state) which is an example of resonant Raman scattering (RRS). In Ni the  $L_3$  excitation is around 853 eV and the Raman photons are around 742 eV; in the metal Co the energies are 778 and 677 eV, respectively. Perpendicular RRS (PRRS) has the potential to give a strong impact on the spectroscopy of magnetic systems for several reasons.

(i) Compared to element-specific techniques based on electron detection, where multiple scattering effects play an important role, photon scattering is much better suited for bulk spectroscopy. It can be carried out on insulators without further complications and is not influenced by external magnetic fields allowing measurements in strong magnetic fields which are not possible with electron detection.

(ii) As we will show below, PRRS has a strong sensitivity to the nature of the valence states although it is based on an inner shell process. In particular, great differences are seen between localized and itinerant systems. PRRS allows one to obtain information not accessible to other spectroscopies as is shown here for Co where some nonbandlike aspects are observed.

(iii) RRS in the soft-x-ray range is becoming accessible on an almost routine basis by exploiting modern synchrotron radiation (SR) sources. Dichroism in PRRS can be measured with only minor modifications of the experimental setup used in valence emission dichroism [6–11] although the experiments are conceptually quite different. Thus, a lot of PRRS information is often left unexplored while it is at hand. The dichroic self-absorption problems [12] limiting the use of resonantly excited valence

fluorescence are totally absent in the present case, allowing a very wide application of PRRS. Although this is important, we stress that the goal of the present Letter is to present an entirely new development and not an alternative path to a method already known.

First, we will demonstrate the feasibility of PRRS for a conceptually simple case. We choose magnetic  $\text{Ni}^{2+}$  ion in Ni ferrite ( $\text{NiFe}_2\text{O}_4$ ) since the ground state, which is approximately  $3d^8$ , is relatively easy to calculate within an ionic approach [13]. From an experimental point of view, however, this choice was less convenient because the Ni signal (around 742 eV) is strongly attenuated by Fe absorption above the  $L_2$  threshold (720 eV). This nondichroic process does not generate artifacts but strongly limits the counting rate. This limitation does not apply to Co which is discussed as a further application where we studied the excitation energy dependence of the scattering. This case cannot be interpreted in a straightforward manner, because neither a localized nor an itinerant picture is *a priori* justified. We observe strong dichroism at the  $L_3$  edge while the integrated dichroism at the  $L_2$  edge disappears within the errors conformed to the theory [3,4]. We found also a dichroism at an excitation energy between both  $L$  edges, a result which cannot be interpreted in a bandlike picture. The Co spectra clearly demonstrate that there are large differences in the results between localized and itinerant systems.

The geometry of the experiment is depicted in Fig. 1. The sample is magnetized along the surface and the scattered photons are detected along the direction  $\mathbf{q}'$  (take-off angle  $\theta$ ). The core hole polarization and the asymmetry in the angular distribution can be understood by considering the following antagonistic effects. On the one hand, spin-orbit interaction prefers the expectation value of the core hole orbital moment to align along its spin direction, which tends to be oriented by the magnetization. On the other hand, the selection rules for optical excitation result in a preferred alignment of the orbital moment parallel to the helicity vector of the circularly polarized light. Both effects are accommodated if the core

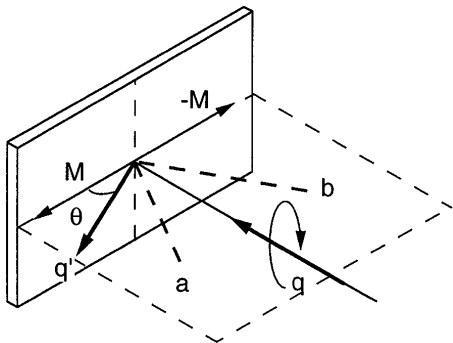


FIG. 1. Schematic geometry of perpendicular resonant Raman scattering. The direction of the incident beam is given by  $\mathbf{q}$  and the detection direction by  $\mathbf{q}'$ . The magnetization  $M$  is in the surface plane.

hole orbital moment is aligned along an intermediate direction which can be represented pictorially by the dashed lines **a** and **b** in Fig. 1 for the two opposite magnetization directions. Therefore, the scattered photon spectrum along an off-normal direction will become different when either the magnetization or the light helicity vector is reversed. Expressed in a more theoretical way [3,4], if one uses a multipolar expansion of the states, the absorption is related to the number of the core holes (the monopole term) while the scattering dichroism integrated over the emitted photon spectrum describes the departure from the spherical symmetry of the space distribution (quadrupole moment which is the core hole polarization).

Measurements were done at beam line ID12B of the European Synchrotron Radiation Facility as in Ref. [10] using a novel incident beam monochromator [14] (1.2 eV bandwidth) except that the light was at normal incidence to the sample (Fig. 1). The detector bandwidth was 1.3 eV. The take-off angle was  $\theta = 20^\circ$ . The Ni ferrite sample was an epitaxially grown crystalline 3 micron film prepared on a MgO single crystal [15]. The Co sample was evaporated *ex situ* (2000 Å) on as grown Si wafer and capped with 20 Å Au; the effect of a possible thin silicide at the Si-Co interface is negligible.

The Ni ferrite results are given in Fig. 2. The  $L_3$  excitation is shown by the arrow in the absorption spectrum [Fig. 2(a)], and the raw scattering data are given in

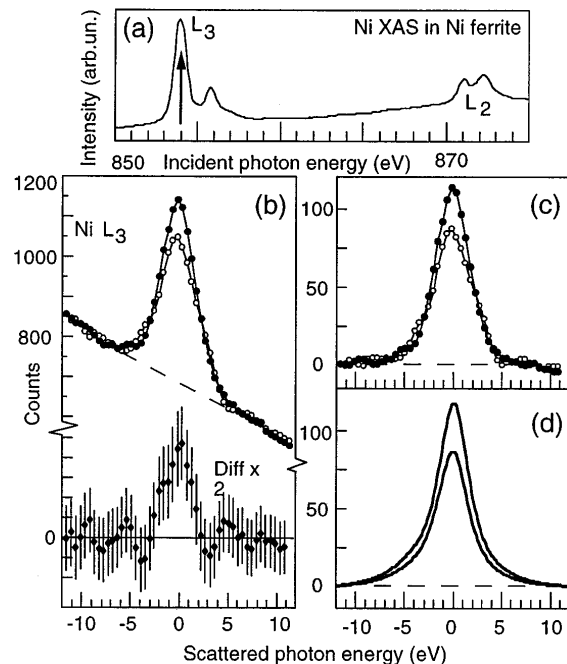


FIG. 2. Perpendicular resonant Raman scattering at Ni  $L_3$  in Ni ferrite. Panel (a):  $L_{2,3}$  absorption (the arrow indicates the excitation energy). Panel (b): Raw scattering data with the energy measured from the peak and difference curve (scale:  $\times 2$ ) corrected for the incident polarization. Panel (c): measurements after polarization correction and background subtraction. Panel (d): Theoretical spectra.

Fig. 2(b) with the energy of the scattered photons measured relative to the peak maximum (final Ni- $3s^1$  state) which is on the decreasing tail of the nonresonant Fe  $L_{2,3}$  signal. The Ni peak height is roughly one-third of the background, and the integrated counting rate is very low (2.6 counts/min) due to self-absorption as mentioned above. A large change in signal occurs when either the polarization or the magnetization is reversed. The difference spectrum in Fig. 2(b) has been corrected for incomplete polarization of the incident beam ( $P = 0.84$ ) and gives, despite the error bars, clear evidence for the dichroism in perpendicular geometry. The Ni peak after polarization correction and background subtraction is shown in Fig. 2(c) with the curves normalized to 100 for the average over both helicities. The background was obtained using a polynomial fit; the fine tuning of the parameters had very little effect on the peak dichroism (28% of the average peak height). The theoretical results are shown in Fig. 2(d) for a calculation performed using the model of Ref. [13] and taking into account the polarization and angles in the matrix elements of the Kramers-Heisenberg formula. The theoretical curves include the effect of bandpasses and the final state lifetime which is the dominant contribution to the broadening. Ligand hole effects were neglected, since their influence is small at Ni $^{2+}$   $L_3$  threshold. We already showed in Ref. [13] that this approach provides an adequate description for the RRS line shape of Ni $^{2+}$  excited at the  $L_3$  peak in NiO, so that we expect it to work also in the present case. The theoretical peak dichroism is 31% consistent with the measured 28% within the experimental accuracy. In fact, at fit of the measurements with a curve having the theoretical shape gives a peak value  $0.28 \pm 0.05$ . This demonstrates the feasibility of PRRS and its application to strongly correlated systems in combination with ionic model calculations, where ligand holes can be included if needed. However, in Ni ferrite the statistics impedes a discussion of the line shape and energy dependence of the observed dichroism. These effects are beyond the purpose of the demonstration experiment on Ni ferrite. In the case of a more complicated final state, which would have been inappropriate as a starting point for this new research, there can be a substantial increase in the counting rate resulting in a reduction of the error bars. For example, in Co ferrite the energy of the transition to Co  $3s^1$  final state is below the Fe edge which can lead to a large increase in the counting rate.

We now proceed by applying PRRS to Co, which, regarding its  $3d$  count between 7 and 8, is close to the preceding case. Admittedly, this metal is a more challenging system since the electron delocalization invalidates a simple atomiclike picture. Co has weak self-absorption in RRS, so that the integrated counting rate (130 counts/min with  $L_3$  excitation) allows us to study the excitation energy dependence. The measured  $L$  edge absorption spectrum is given in Fig. 3(a) with the arrows indicating the

excitation energies. The corresponding scattering results are given in Figs. 3(b), 3(c), and 3(d) where the difference curves have been corrected for the polarization of the incident light ( $P = 0.82$ ). The energies of the scattering light are measured from the peak of the signal measured with  $L_3$  excitation. We restrict ourselves to mention only the most interesting points about the spectra.

(i) Comparison between the excitation at the  $L_3$  and  $L_2$  edges. Since core multipoles above the monopole exist only for a core state of total angular momentum larger than  $j = 1/2$  (Ref. [4]), the dichroism integrated on the scattered photon energy should vanish at the  $L_2$  edge. The measured integrated dichroism at the  $L_3$  edge [Fig. 3(b)] is  $(11.5 \pm 0.6)\%$ , while at the  $L_2$  edge [Fig. 3(d)] the integrated dichroism is  $(0.3 \pm 1.4)\%$ . Thus, within the accuracy, the  $L_2$  dichroism vanishes, which provides a strong support for the theoretical picture. We note that, because of the large  $2p$ - $3d$  Coulomb and exchange interactions,  $j$  is not an exact quantum number, therefore, a small integrated dichroism can still be present at the

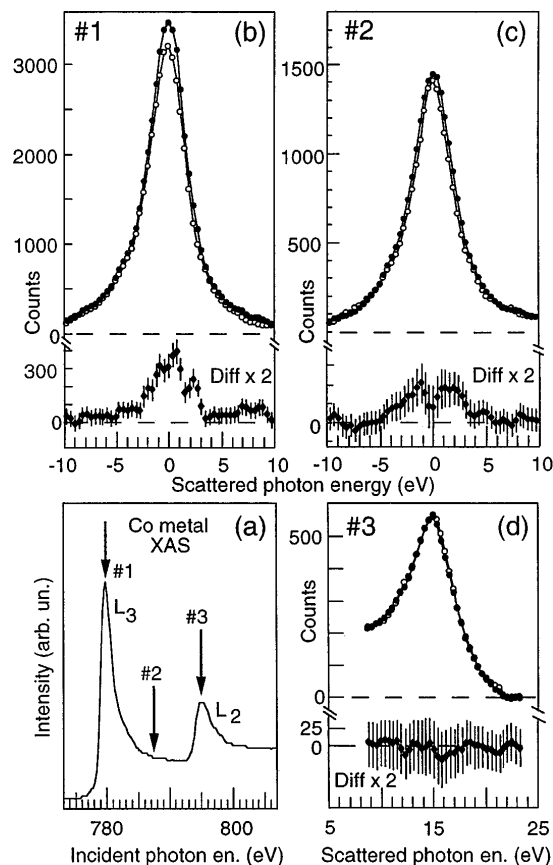


FIG. 3. Perpendicular resonant Raman scattering measurements for Co metal. Panel (a):  $L_{2,3}$  absorption with the arrows indicating the excitation energies. Scattering results with  $L_3$  peak excitation [panel (b)], with excitation 7.5 eV above  $L_3$  [panel (c)], and with  $L_2$  peak excitation [panel (d)]. The difference curves (scale:  $\times 2$ ) are corrected for the incident polarization. The energies are measured from the peak measured with  $L_3$  excitation.

$L_2$  edge. The existence of such a small effect should be kept in mind. Despite their difficulty these measurements might become technically feasible on a routine basis in the near future.

(ii) Comparison between the magnitude of the dichroism in Ni ferrite and Co at the  $L_3$  resonance. The observed dichroism in Co is about a factor of 3 smaller. There can be several reasons for such a reduction in itinerant materials. In an ionic compound, such as Ni ferrite, the valence hole spin polarization  $P = [n(\uparrow) - n(\downarrow)]/[n(\uparrow) + n(\downarrow)]$  will be close to 1, whereas in Co  $P$  can be as low as 0.65 as suggested by the MCXD sum rule [16], and line shape analysis [17]. According to Refs. [4,18], the core hole quadrupole moment is primarily determined by the spin moment in the ground state with the orbital moment and magnetic dipole term playing a far less important role. Thus, the diminished valence hole spin polarization in Co can account at most for a reduction to  $\frac{2}{3}$  compared to Ni ferrite; i.e., it is not sufficient to explain the measured effect. This argument is affected only marginally by the possible modification of the sum rules in itinerant systems since the nonatomic effects in  $3d$  TMS sum rules are evaluated [19] to be typically around 10%. A further reduction can be caused by the mixing between the intermediate state configurations, such as  $2p^53d^8$ ,  $2p^53d^9$ , and  $2p^53d^{10}$ , which reduces the quadrupole moment. In itinerant metals this mixing is much larger than in localized systems. It is interesting to mention that a similar reduction in the dichroism has also been observed for Fe, Co, and Ni metal in perpendicular resonant  $2p3p3p$  photoemission [3,18]. This emphasizes the importance of further investigations using perpendicular spectroscopies on systems with varying valence electron localization.

(iii) For an excitation 7.5 eV above the  $L_3$  peak (case #2 of Fig. 3) there is still a considerable dichroism [maximum dichroism  $(6.8 \pm 1)\%$  against  $(10.4 \pm 1.5)\%$  at  $L_3$ ]. At these excitation energies it is generally believed that the excitation is not to empty  $3d$  states but to  $(sp)$  itinerant bandlike states. The present dichroism in PRRS is about  $\frac{2}{3}$  of the effect at the  $L_3$  peak, which is too high for dipole transitions to  $(sp)$  itinerant valence states, which give an almost negligible absorption dichroism and, in band calculations, a very small spin polarization.

This suggests the presence of a significant amount of  $2p^53d^{n+1}$  states well above the excitation threshold in the intermediate state, a presence obviously not compatible with a bandlike behavior. This would give support to results obtained by Anderson impurity calculations [20].

In summary, we can say that resonant inner shell scattering excited with circularly polarized x rays in perpendicular geometry offers new possibilities to study the valence states of magnetic  $3d$  transition metal systems. Despite the fact that the scattering process involves an inner shell excitation in the final state, there is a strong sensitivity for the valence electronic structure.

- 
- [1] See, e.g., *Spin-Orbit Influenced Spectroscopies of Magnetic Solids*, edited by H. Ebert and G. Schutz (Springer-Verlag, Berlin, 1996).
  - [2] B. T. Thole *et al.*, Phys. Rev. Lett. **68**, 1943 (1992).
  - [3] B. T. Thole, H. A. Dürr, and G. van der Laan, Phys. Rev. Lett. **74**, 237 (1995).
  - [4] G. van der Laan and B. T. Thole, J. Phys. Condens. Matter **7**, 9947 (1995).
  - [5] H. A. Dürr, G. van der Laan, and M. Surman, J. Phys. Condens. Matter **8**, L7 (1996).
  - [6] P. Strange, P. J. Durham, and B. L. Gyorffy, Phys. Rev. Lett. **67**, 3590 (1991).
  - [7] C. F. Hague *et al.*, Phys. Rev. B **48**, 3560 (1993).
  - [8] L.-C. Duda *et al.*, Phys. Rev. B **50**, 16758 (1994).
  - [9] C. F. Hague *et al.*, Phys. Rev. B **51**, 1370 (1995).
  - [10] L. Braicovich *et al.*, Phys. Rev. B **55**, R14729 (1997).
  - [11] S. Eisebitt *et al.*, Solid State Commun. **104**, 173 (1997).
  - [12] L. Braicovich *et al.*, Solid State Commun. **105**, 264 (1998).
  - [13] L. Braicovich *et al.*, Phys. Rev. B **55**, R15989 (1997).
  - [14] G. Ghiringhelli *et al.*, Rev. Sci. Instrum. **69**, 1610 (1998).
  - [15] E. Z. Katsnelson, A. G. Karoza, and M. M. Chervinskii, Phys. Status Solidi (a) **111**, K233 (1989).
  - [16] C. T. Chen *et al.*, Phys. Rev. Lett. **75**, 152 (1995).
  - [17] G. van der Laan, Phys. Rev. B **55**, 8086 (1997).
  - [18] G. van der Laan *et al.*, J. Electron Spectrosc. Relat. Phenom. **78**, 213 (1996).
  - [19] P. Carra, Contribution to the VUV12 Conference, San Francisco, 1998.
  - [20] G. van der Laan and B. T. Thole, J. Phys. Condens. Matter **4**, 4181 (1992).